Molecular Therapy
Methods & Clinical Development
Original Article

SERCA2a overexpression improves muscle function in a canine Duchenne muscular dystrophy model

Kasun Kodippili,[1,7] Chady H. Hakim,[1,7] Matthew J. Burke,[1] Yongping Yue,[1] James A. Teixeira,[1] Keqing Zhang,[1] Gang Yao,[2] Gopal J. Babu,[3] Roland W. Herzog,[4] and Dongsheng Duan[1,2,5,6]

[1]Department of Molecular Microbiology and Immunology, School of Medicine, The University of Missouri, Columbia, MO 65212, USA; [2]Department of Chemical and Biomedical Engineering, College of Engineering, The University of Missouri, Columbia, MO 65212, USA; [3]Department of Cell Biology and Molecular Medicine, Rutgers New Jersey Medical School, Newark, NJ 07103, USA; [4]Herman B Wells Center for Pediatric Research, Indiana University, Indianapolis, IN 46202, USA; [5]Department of Neurology, School of Medicine, The University of Missouri, Columbia, MO 65212, USA; [6]Department of Biomedical Sciences, College of Veterinary Medicine, The University of Missouri, Columbia, MO 65212, USA

Excessive cytosolic calcium accumulation contributes to muscle degeneration in Duchenne muscular dystrophy (DMD). Sarco/endoplasmic reticulum calcium ATPase (SERCA) is a sarcoplasmic reticulum (SR) calcium pump that actively transports calcium from the cytosol into the SR. We previously showed that adeno-associated virus (AAV)-mediated SERCA2a therapy reduced cytosolic calcium overload and improved muscle and heart function in the murine DMD model. Here, we tested whether AAV SERCA2a therapy could ameliorate muscle disease in the canine DMD model. 7.83×10^{13} vector genome particles of the AAV vector were injected into the extensor carpi ulnaris (ECU) muscles of four juvenile affected dogs. Contralateral ECU muscles received excipient. Three months later, we observed widespread transgene expression and significantly increased SERCA2a levels in the AAV-injected muscles. Treatment improved SR calcium uptake, significantly reduced calpain activity, significantly improved contractile kinetics, and significantly enhanced resistance to eccentric contraction-induced force loss. Nonetheless, muscle histology was not improved. To evaluate the safety of AAV SERCA2a therapy, we delivered the vector to the ECU muscle of adult normal dogs. We achieved strong transgene expression without altering muscle histology and function. Our results suggest that AAV SERCA2a therapy has the potential to improve muscle performance in a dystrophic large mammal.

INTRODUCTION

Duchenne muscular dystrophy (DMD) is a severe and progressive muscle disorder caused by null mutations in the X-linked *DMD* gene.[1] This results in the loss of the sub-sarcolemmal protein dystrophin. Dystrophin maintains sarcolemmal stability by establishing a structural link between the cytoskeleton and the extracellular matrix. Although weakened sarcolemmal integrity is the primary defect in DMD, impaired calcium homeostasis has also been implicated in DMD pathogenesis.[2–4] Elevated cytosolic calcium triggers protein degradation and membrane damage by activating calcium-dependent calpain protease and phospholipase.

A primary contributor to the cytosolic calcium overload in DMD is the ineffective removal of calcium from the cytosol. Sarco/endoplasmic reticulum (SR) calcium ATPase (SERCA) is responsible for greater than 70% of calcium removal in muscle cells.[2,5] SERCA belongs to the family of P-type ATPases and consists of a single polypeptide of about 110 kDa. SERCA utilizes the energy of ATP hydrolysis to transport calcium from the cytosol into the lumen of the SR, across an almost 10,000-fold concentration gradient.[6] SERCA activity is significantly reduced in dystrophin-deficient muscles.[2]

More than 10 distinct isoforms of SERCA have been identified. SERCA2a is expressed in skeletal, cardiac, and smooth muscles but not in non-muscle cells.[5] We have previously explored adeno-associated virus (AAV)-mediated SERCA2a overexpression in the mdx mouse model of DMD.[7,8] In aged mdx mice, AAV SERCA2a delivery significantly improved the electrocardiographic performance.[7] When the AAV SERCA2a vector was delivered to 3-month-old mdx mice, we observed a significant improvement in grip force, treadmill running, electrocardiography, and cardiac hemodynamics.[8]

While the data from mdx mice are highly promising, it is unclear whether SERCA2a therapy can be translated to a dystrophic large mammal. The canine model has been extensively used to evaluate AAV gene therapy for DMD.[9–13] Unlike mdx mice, affected dogs display a severe clinical phenotype more comparable to that of human patients.[14] Here, we delivered an AAV SERCA2a vector to four affected dogs by intramuscular injection to the extensor carpi ulnaris (ECU) muscle. Compared to excipient-injected muscle, AAV-mediated SERCA2a overexpression significantly enhanced

Received 15 February 2024; accepted 16 May 2024;
https://doi.org/10.1016/j.omtm.2024.101268.

[7]These authors contributed equally

Correspondence: Dongsheng Duan, PhD, Department of Molecular Microbiology and Immunology, School of Medicine, The University of Missouri, Columbia, MO 65212, USA.
E-mail: duand@missouri.edu

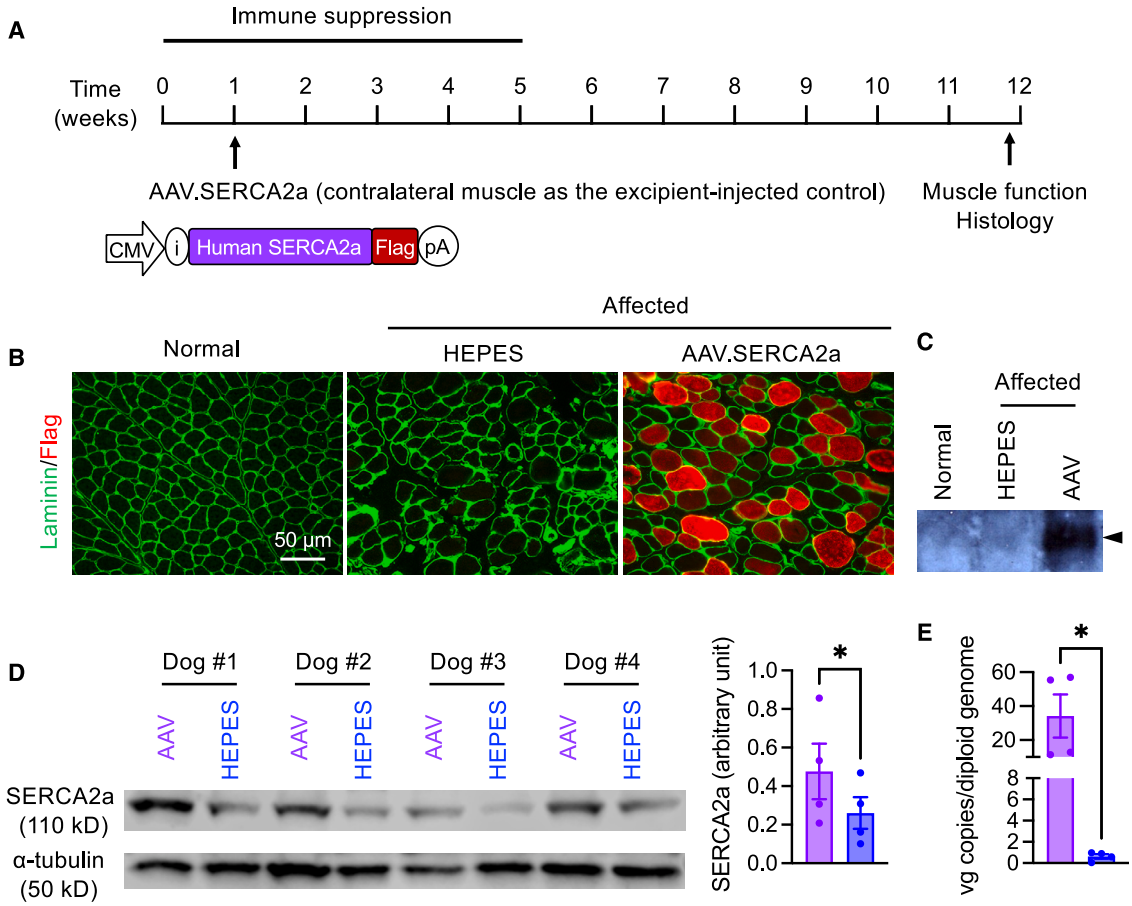

Figure 1. AAV therapy increased SERCA2a expression in the canine model of Duchenne muscular dystrophy

(A) Schematic illustration of the study plan. Transient immune suppression was applied for 5 weeks starting 1 week before AAV injection. The AAV.SERCA2a vector was injected into one side of the extensor carpi ulnaris muscle (ECU) in four juvenile affected dogs. The contralateral ECU muscle received an equal volume of the excipient (HEPES buffer). Muscle function and histology were evaluated at the ~12 weeks time point. The cartoon illustrates the expression cassette of the AAV.SERCA2a vector. i, intron in the expression cassette. (B) Representative immunofluorescence staining images for laminin and the transgene-specific FLAG tag in the muscles of a normal dog and an affected dog that received AAV.SERCA2a (one side of the ECU muscle) and HEPES buffer (contralateral side of the ECU muscle). (C) Representative FLAG tag western blot from a normal dog and an affected dog that received AAV.SERCA2a (one side of the ECU muscle) and HEPES buffer (contralateral side of the ECU muscle). Arrowhead, FLAG tag (110 kD). (D) Western blot evaluation of SERCA2a expression from AAV.SERCA2a-injected and contralateral HEPES buffer-injected ECU muscles of all four affected dogs used in the study. α-Tubulin is the loading control. Densitometry analysis shows SERCA2a protein level quantification. Error bar, standard error of the mean. *$p < 0.05$. SERCA2a, sarco/endoplasmic reticulum calcium ATPase 2a; HEPES, N-2-hydroxyethylpiperazine-N-2-ethane sulfonic acid. (E) Quantification of the AAV vector genome (vg) copy number. Error bar, standard error of the mean. *$p < 0.05$.

SR calcium uptake, reduced calpain activity, and improved contractile kinetics and eccentric contraction performance. Nonetheless, muscle histology was not improved. We further showed that SERCA2a overexpression did not induce untoward responses in normal dog muscle.

RESULTS

Intramuscular delivery resulted in widespread human SERCA2a expression in the ECU muscle of affected dogs

We first examined SERCA2a expression in the ECU muscle of normal and affected dogs (Figure S1). Upon immunostaining, SERCA2a-expressing myofibers were greatly reduced in the affected dog muscle (Figure S1A). In the western blot, the SERCA2a levels in normal and affected dog muscles were 0.62 ± 0.07 and 0.25 ± 0.07, respectively. SERCA2a expression in normal muscles was significantly higher (2.48-fold) than that of affected muscles (Figure S1B).

To evaluate SERCA2a gene therapy in dystrophic dog muscle, we packaged a FLAG-tagged human SERCA2a construct into Y371F AAV9 and delivered the vector to one side of the ECU muscle of four mixed-breed female affected dogs at a dose of 7.83×10^{13} vector genome (vg) particles/muscle (Figure 1A). The contralateral ECU muscle received the excipient (HEPES buffer) at the same volume. To minimize vector-induced immune rejection, we applied transient immunosuppression for 5 weeks using cyclosporine and

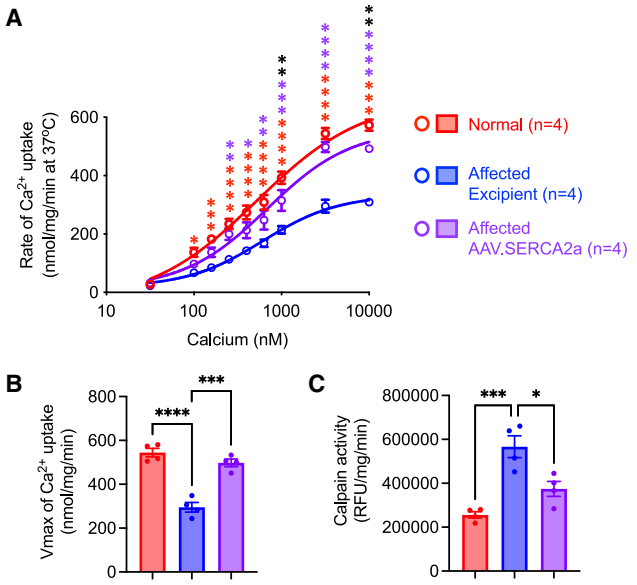

Figure 2. AAV.SERCA2a injection improved calcium uptake by the SR and reduced cytosolic calpain activity

(A) Tracing of SR calcium-dependent calcium uptake in the ECU muscle of normal dogs and affected dogs that received AAV.SERCA2a and excipient. Statistical differences between normal and excipient-injected affected dogs are marked with red asterisks. Statistical differences between AAV.SERCA2a-injected and excipient-injected affected dogs are marked with purple asterisks. Statistical differences between normal and AAV.SERCA2a-injected affected dogs are marked with black asterisks. (B) The maximum rate of SR calcium uptake (Vmax) in the ECU muscle of normal dogs and affected dogs that received AAV.SERCA2a and excipient. (C) Quantification of cytosolic calpain activity in the ECU muscle of normal dogs (n = 4) and affected dogs that received AAV.SERCA2a on one side of the ECU muscle (n = 4) and excipient on the contralateral ECU muscle (n = 4). RFU, relative fluorescence unit. Error bar, standard error of the mean. $^{*}p < 0.05$, $^{**}p < 0.01$, $^{***}p < 0.001$, and $^{****}p < 0.0001$.

mycophenolate mofetil using our published protocol.[15] Three months following gene transfer, we evaluated transgene expression, SR calcium uptake, and muscle histology and function.

Upon immunostaining using an antibody against the FLAG tag, we observed widespread expression in AAV-injected muscles (Figures 1B and S2). Contralateral excipient-injected muscles did not show FLAG expression. The FLAG expression in AAV-injected muscle was confirmed by western blot (Figure 1C). We quantified total SERCA2a expression by western blot (Figure 1D). The SERCA2a levels in AAV-treated and excipient-injected muscles were 0.48 ± 0.14 and 0.26 ± 0.08, respectively. SERCA2a expression in AAV-treated muscles was significantly higher (1.85-fold) than that of excipient-injected muscles (Figure 1D), suggesting that AAV therapy improved but did not normalize SERCA2a expression. Consistent with immunostaining and western blot results, we detected 34.14 ± 12.72 copies/diploid genome of the vector genome in AAV-injected muscles (Figure 1E). The AAV genome was barely detected in excipient-injected muscles (0.62 ± 0.21 copies/diploid genome) (Figure 1E).

SERCA2a overexpression improved SR calcium uptake and reduced calpain activity in AAV-injected muscles

Compared to excipient-injected muscle, the rate of calcium uptake was significantly enhanced in AAV-injected muscles, although it did not reach normal levels (Figure 2A). Consistently, the maximum rate of SR calcium uptake was significantly increased in AAV-injected muscles (Figure 2B). Quantification of cytosolic calpain activity revealed a significant reduction in AAV-injected muscles (Figure 2C).

SERCA2a overexpression did not improve muscle histology or myofiber-type composition

To determine whether increased SERCA2a expression ameliorated muscle pathology, we quantified the percentage of centrally nucleated myofibers, a marker for regeneration. No difference was detected between AAV-injected and excipient-injected muscles (Figure 3A). We examined muscle fibrosis by Masson trichrome staining (Figures 3B and S3). AAV-injected and excipient-injected muscles showed similar levels of fibrosis. We also did not find differences in myofiber size distribution between AAV-injected and excipient-injected muscles (Figure 3C). Next, we examined myofiber-type composition (Figure 3D). Compared to excipient-injected muscles, there was a trend toward fewer type IIa fibers and more type I fibers and type I/IIa hybrid fibers in AAV-injected muscles. However, these differences did not reach statistical significance (Figure 3D).

Human SERCA2a expression induced FoxP3+ T cell infiltration

To determine whether human SERCA2a expression led to the cytosolic T lymphocyte response in the canine muscle, we evaluated the infiltration of CD4+ T cells and CD8+ T cells in the ECU muscle by immunohistochemistry staining (Figure 4). In excipient-injected muscle, we only detected a few residential T cells. However, we detected abundant T cell infiltration in AAV-injected muscle, which was accompanied by FoxP3+ nuclear staining.

SERCA2a overexpression improved contractile kinetics and enhanced resistance to eccentric-contraction-induced force decline

To evaluate the physiological consequences of SERCA2a overexpression in dystrophic muscle, we performed the *in situ* force assay using our published protocol (Figure 5).[16,17] No differences were detected in the anatomic properties of the ECU muscle (weight, length, and physiological cross-sectional area [pCSA]) between AAV- and excipient-injected muscles (Table 1). The absolute and specific twitch forces were 5.94 ± 0.77 N and 0.82 ± 0.10 N/cm^2 in AAV-injected muscles, respectively, and 5.89 ± 0.34 N and 0.79 ± 0.07 N/cm^2 in excipient-injected muscles, respectively. There were no significant differences. Interestingly, the time to peak tension and the half-relaxation time were significantly prolonged in AAV-injected muscles (Figures 5A and 5B; Table S2). Similar to the twitch forces, SERCA2a overexpression did not change the tetanic forces (Figures 5C and 5D). Dystrophin-deficient muscle is particularly susceptible to injury caused by eccentric contraction where the contracting muscle is lengthened by external force.

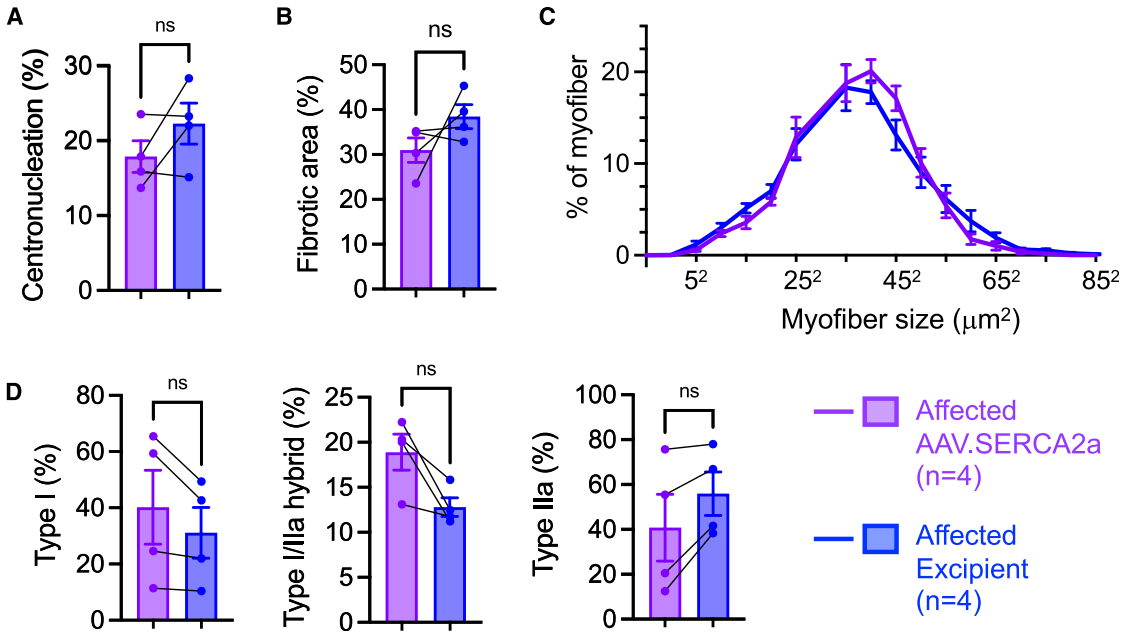

Figure 3. Muscle histology in AAV.SERCA2a-injected and contralateral excipient-injected muscle of affected dogs

(A) Quantification of myofibers with centrally located nuclei. (B) Quantification of the fibrotic area. (C) Quantification of myofiber size (cross-sectional area) distribution. (D) Quantification of myofiber type. Error bar, standard error of the mean. ns, $p > 0.05$.

SERCA2a overexpression significantly protected the ECU muscle from eccentric-contraction-induced force loss (Figure 5E).

SERCA2a overexpression did not alter muscle histology or function in adult normal dogs

Next, we examined SERCA2a overexpression in mixed-breed normal male dogs (Figure 6). We delivered that same dosage of the SERCA2a vector to the ECU muscle of three normal dogs. FLAG tag immunofluorescence staining showed strong gene transfer (Figure 6A). H&E and Masson trichrome staining showed normal morphology and a lack of fibrosis (Figure 6A). We compared the anatomic and contractile properties of AAV-injected muscles with untreated normal muscles (Table 2; Figures 6B–6F). No statistically significant differences were detected in any parameters including muscle weight and length, pCSA, contraction kinetics, absolute and specific forces, and eccentric contraction profiles.

DISCUSSION

In this study, we evaluated SERCA2a overexpression therapy in the canine DMD model by intramuscular injection of a human SERCA2a AAV vector in the ECU muscle. We first showed that SERCA2a expression was reduced in affected dogs (Figure S1). We then designed a paired study with one side of the muscle receiving the SERCA2a vector and the other side receiving the excipient. We achieved widespread transgene expression that was accompanied by FoxP3+ T cell infiltration, suggesting a regulatory T cell response in transduced muscle (Figures 1, 4, and S2). We observed an elevation of the SERCA2a level in AAV-injected muscles (Figure 1D). SERCA2a overexpression increased SR calcium uptake and diminished calpain activity but did not mitigate muscle pathology (Figures 2, 3, and S3). Nonetheless, SERCA2a overexpression significantly protected dystrophic muscle from eccentric-contraction-induced force loss (Figure 5). We also delivered the same SERCA2a vector to the normal ECU muscle and did not detect any change in muscle histology or function (Figure 6).

The abnormal elevation of cytosolic calcium is a major pathogenic determinant of DMD.[2] Restoration of calcium homeostasis has emerged as a highly promising therapeutic strategy for DMD. Various pharmaceutic approaches have been explored, such as blocking calcium entry from the sarcolemma,[18] preventing calcium leak from the SR,[19] and enhancing calcium uptake by the SR.[20] Several groups have also evaluated gene therapy as a strategy to improve SR calcium recycling in murine models of muscular dystrophy.[7,21–24] Morine et al. delivered SERCA1a to newborn mdx mice using AAV1 and observed a significant improvement in diaphragm histology and function.[21] Goonasekera et al. showed an improvement in muscle morphology by injecting an AAV9 SERCA2a vector into the gastrocnemius muscle of neonatal δ-sarcoglycan knockout mice, a model for limb girdle muscular dystrophy.[22] We demonstrated significant amelioration of the cardiac phenotype in aged mdx mice with systemic AAV9 SERCA2a delivery.[7,8] In addition to AAV-mediated SERCA delivery, targeting SERCA regulators also yielded promising results in mouse DMD models. Specifically, AAV-mediated knockdown of sarcolipin, a negative SERCA regulator, significantly extended the lifespan of the severe dystrophin/utrophin double-knockout mice.[23] AAV-mediated overexpression of Dwarf open

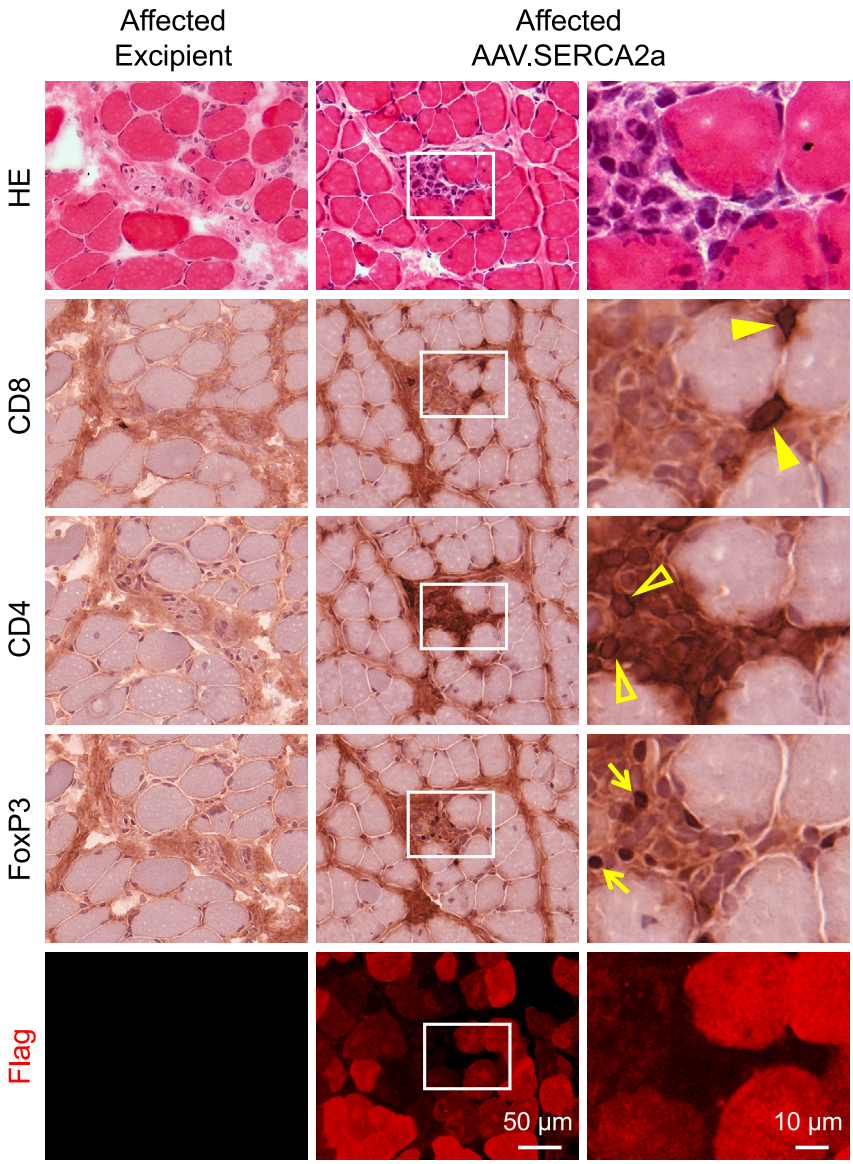

Figure 4. Evaluation of the T cell response in AAV.SERCA2a-injected and contralateral excipient-injected muscle of affected dogs

Representative photomicrographs of H&E staining, CD8 (a marker for cytotoxic T cells), CD4 (a marker for helper T cells), and FoxP3 (a marker for regulatory T cells) immunohistochemistry staining and FLAG tag immunofluorescence staining. Right-column photomicrographs are high-magnification images of the boxed areas in the corresponding middle-column photomicrographs. Filled arrowhead, CD8+ T cells; open arrowhead, CD4+ T cells; arrow, FoxP3+ nuclei.

reading frame, a positive SERCA regulator, ameliorated cardiomyopathy in aged mdx mice.[24] Collectively, a large body of evidence in murine models supports further evaluation of SERCA-based gene therapy in large animal models.

We started with evaluating SERCA2a expression in the ECU muscle of normal and affected dogs. It has been shown that the SERCA2a level was reduced in the quadriceps of patients with DMD.[23] Intriguingly, SERCA2a expression was upregulated in the quadriceps of mdx mice.[25] We found a significant reduction of the SERCA2a level in affected dogs (Figure S1). Our results in the canine model are consistent with those in human patients. This observation reinforces the relevance of dystrophin-deficient dogs as a valid model for translational studies.

We have previously established a technique to achieve saturated AAV transduction in the ECU muscle.[9,12] We have also developed methods to study histological and physiological outcomes in the ECU muscle.[17,26] As an initial attempt to test SERCA2a therapy, we performed the study in the ECU muscle. This allows us to test the therapeutic effect with a small amount of vector before mounting a much more expensive systemic delivery study. Further, the contralateral muscle can serve as a control in the same animal.

In this study, we used a vector that expressed human SERCA2a from the ubiquitous cytomegalovirus (CMV) promoter because (1) this vector has been extensively tested in clinical trials,[27–29] (2) we have achieved the proof-of-principle data in mdx mice with this vector,[7,8] and (3) others have tested human SERCA2a AAV vectors in canine models of heart failure by intramyocardial injection.[30,31] A potential concern about using the human cDNA in a canine study is the induction of the cytotoxic T cell response to the human protein.[31–33] We applied transient immune suppression with cyclosporine and mycophenolate mofetil.[15] Persistent transgene expression was observed despite infiltration of CD4+ and CD8+ T cells (Figures 1, 4, and S2). The induction of FoxP3+ regulatory T cells may have helped preserve transgene expression (Figure 4).[34,35] We would like to point out that the CMV promoter is not desirable for clinical translation because it may lead to untoward expression in non-muscle cells and contribute to the cellular response. A muscle-specific promoter should be used in the future development of AAV SERCA2a therapy for DMD.

Consistent with our mdx mouse study, human SERCA2a expression increased the SERCA2a level and SR calcium uptake in AAV-injected muscles (Figures 1 and 2).[8] A downstream event of cytosolic calcium imbalance is the activation of calcium-dependent calpain proteases.[36] Calpain-activation-induced proteolysis contributes to muscle damage in DMD.[37–39] We found that SERCA2a overexpression significantly

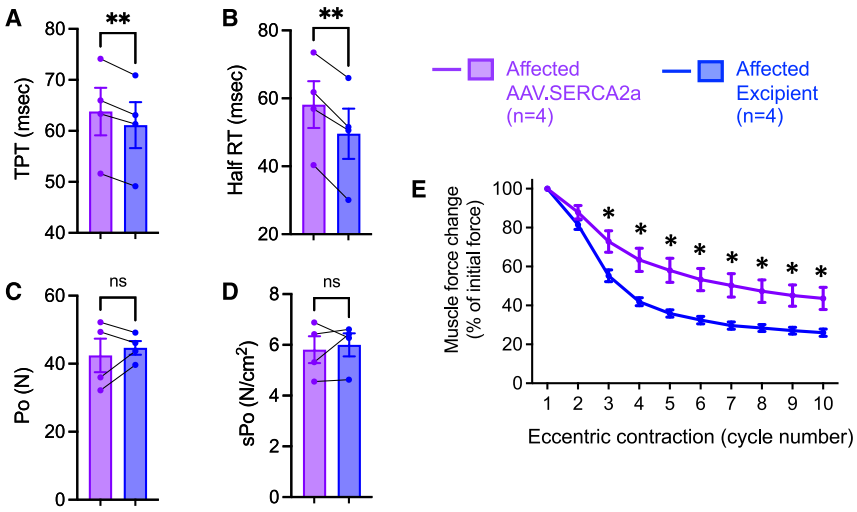

Figure 5. AAV.SERCA2a injection improved the kinetic properties of twitch contraction and resistance to eccentric contraction-induced muscle force decline in affected dogs

(A) Quantification of time to peak tension (TPT) of twitch contraction. (B) Quantification of half-relaxing time (Half RT) of twitch contraction. (C) Quantification of total tetanic muscle force (Po). (D) Quantification of specific tetanic muscle force (sPo). (E) Relative changes of the tetanic force during ten cycles of eccentric contraction. The tetanic force at the beginning of the first cycle of eccentric contraction was designated as 100%. Error bar, standard error of the mean. *$p < 0.05$, **$p < 0.01$, and ns, $p > 0.05$.

reduced calpain activity (Figure 2C). Surprisingly, there was no improvement in histological biomarkers of muscle disease (Figures 3 and S3). One possible explanation is the timing of the SERCA therapy. We treated young adult affected dogs. SERCA therapy may prevent muscle damage before the onset of the disease but cannot rescue existing pathology. In support of this, neonatal AAV SERCA delivery dramatically reduced dystrophic pathology.[21,22] However, we failed to detect histological improvements in skeletal muscle when we delivered the AAV SERCA2a to 3-month-old mdx mice.[8] Another possibility is that calpain inhibition alone was insufficient to ameliorate muscle disease. Indeed, pharmacological calpain inhibition did not result in beneficial changes in murine or canine DMD models.[40,41]

To study the physiological consequences of AAV SERCA2a therapy, we compared muscle function between AAV-injected and contralateral excipient-injected muscles (Figure 5; Table 1). We recently showed that the time to peak tension and the half-relaxing time were significantly shortened in the ECU muscle of affected dogs.[16] We also found that the change in contractile kinetics was associated with a slow to fast myofiber-type switch.[16] AAV SERCA2a therapy significantly increased the time to peak tension and the half-relaxing time (Figures 5A and 5B). Although we did not detect a significant difference in myofiber-type composition between AAV-injected and excipient-injected muscles, the number of slower fibers (type I and type I/IIa hybrid) appeared to be increased while the number of fast fibers (type II) appeared to be decreased following AAV SERCA2a therapy (Figure 3D).

We quantified the absolute and specific tetanic muscle forces but found no significant differences between SERCA2a-treated and excipient-treated muscles (Figures 5C and 5D). Failure to sustain muscle force upon eccentric contraction is a highly sensitive physiological biomarker for dystrophic muscle.[42] Therefore, we challenged the ECU muscle with repeated rounds of eccentric contraction. AAV-injected muscles significantly outperformed excipient-injected muscles (Figure 5E). The lack of improvement in tetanic muscle force is unexpected given that we have previously observed enhanced grip strength and treadmill running in mdx mice with AAV SERCA2a therapy.[8] The exact reason for this discrepancy is unclear but may relate to model differences (mdx limb muscles are less affected). The diaphragm is the only muscle that displays patient-like disease in young mdx mice.[43] AAV-mediated SERCA1a overexpression in the mdx diaphragm partially protected eccentric contraction-induced force loss but did not improve tetanic force.[21] Together, these results suggest that SERCA overexpression alone may only offer limited protection in severely affected muscles. Combinatory therapy (e.g., with dystrophin gene replacement) may be necessary to achieve more effective disease amelioration.

Toxicity associated with transgene overexpression is an important consideration in the development of gene therapy. Two studies suggest that supraphysiological SERCA activation may result in toxic responses.[44,45] Bish et al. delivered short hairpin RNA to knock down phospholamban, a negative SERCA regulator, in the dog heart. The treatment resulted in serum troponin elevation and cardiac function depression.[44] Law et al. found that genetic ablation of phospholamban in mdx mice led to unregulated calcium cycling and worsened cardiac disease.[45] Given these concerns, we delivered the AAV SERCA2a vector to the ECU muscle of normal dogs. Despite strong transgene expression, we saw no abnormality in histology or force measurements (Figure 6; Table 2). Our results were in line with the safety profile in AAV SERCA2a clinical trials.[27–29] The discrepancy between our data and those of Bish et al. and Law et al. may, in part, be due to the strategies used (SERCA2a overexpression versus phospholamban inhibition).

In our studies, we used mixed-breed dogs to better mimic the genetic background of the human population. Due to the availability of dogs, only female affected dogs were used in the AAV SERCA2a therapy study, and only normal male dogs were used in the toxicity study. Future studies using dogs of the opposite sex will illustrate whether gender influences the outcomes of AAV-mediated SERCA2a delivery in dog muscles.

In summary, our study suggests that AAV SERCA2a overexpression can provide some physiological benefits in dystrophic dog muscles

Table 1. Characterization of the ECU muscle of affected dogs

		AAV.SERCA2a injected			Excipient injected		
Dog number	Dog body weight (Kg)	Weight (g)	Length (cm)	PCSA (cm^2)	Weight (g)	Length (cm)	PCSA (cm^2)
#1	13.6	4.43	14.50	7.57	4.58	14.50	7.83
#2	11.6	3.29	13.50	6.04	3.36	13.50	6.17
#3	11.4	4.30	13.50	7.89	5.14	13.50	9.43
#4	13.6	4.49	14.50	7.67	4.08	14.50	6.97

PCSA, physiological cross-sectional area.

without safety concerns. Additional studies are needed to determine (i) whether more protection can be achieved by initiating treatment before the onset of the disease and/or by combining with other genetical therapies, and (ii) whether systemic delivery can lead to body-wide improvement and cardiac function enhancement in the canine DMD model.

MATERIALS AND METHODS

Experimental animals

All animal experiments were approved by the Animal Care and Use Committee of the University of Missouri and were performed in accordance with National Institutes of Health guidelines. All experimental dogs were of a mixed genetic background of golden retriever, Labrador retriever, beagle, spaniel, and Welsh corgi and were generated in-house by artificial insemination. A total of 18 dogs were used in the study, including four affected dogs and 14 normal dogs (Table S1). The genotype was determined by polymerase chain reaction according to published protocols.[46,47] The diagnosis was further confirmed by the serum creatine kinase levels, clinical presentations, and muscle pathology. The affected dogs carry null mutations in the dystrophin gene. Specifically, affected dog #1 carried the golden retriever muscular dystrophy (GRMD) mutation (a point mutation in intron 6) in one X chromosome and the Labrador retriever muscular dystrophy (LRMD) mutation (an insertion in intron 19) in the other X chromosome. Affected dog #2 carried the GRMD mutation in one X chromosome and the Welsh corgi muscular dystrophy (WCMD) mutation (an insertion in intron 13) in the other X chromosome. Affected dogs #3 and #4 carried the LRMD mutation in one X chromosome and the WCMD mutation in the other X chromosome. These mutations abolished dystrophin expression.

All experimental dogs were housed in a specific-pathogen-free animal care facility and kept under a 12 h light/12 h dark cycle. Affected dogs were housed in a raised platform kennel, while normal dogs were housed in a regular floor kennel. Depending on the age and size, two or more dogs were housed together to promote socialization. Normal dogs were fed with dry Purina Laboratory Canine Diet 5006 (LabDiet, St. Louis, MO, USA, #0001324), while affected dogs were fed with wet Purina Pro Plan Puppy food as instructed by the veterinarian (Purina Pro Plan Puppy dry and canned food, #38100-02773). Dogs were given *ad libitum* access to clean drinking water. Toys were allowed in the kennel with dogs for activity enrichment. Dogs were monitored daily by the caregivers for overall health condition and activity. A complete physical examination was performed by the veterinarian from the Office of Animal Research at the University of Missouri for any unusual changes in behavior, activity, food and water consumption, or clinical symptoms. The body weights of the dogs were measured periodically to monitor growth and body condition. Experimental subjects were euthanized at the end of the study according to the 2013 American Veterinary Medical Association Guidelines for the Euthanasia of Animals.

Recombinant Y731F tyrosine mutant AAV9 SERCA2a vector production

The *cis*-plasmid for SERCA2a vector production was published before.[8] In this construct, the human SERCA2a cDNA expression was regulated by the ubiquitous CMV promoter, a hybrid intron, and a bovine growth hormone poly-adenylation signal. The Y731F tyrosine mutant AAV9 packaging plasmid was published before.[10,48] The experimental AAV vector was produced using a triple plasmid transfection protocol as previously described.[49] Recombinant viral stocks were purified through three rounds of CsCl ultracentrifugation followed by two rounds of dialysis in HEPES (N-2-hydroxyethylpiperazine-N-2-ethane sulfonic acid) buffer (excipient) according to our published protocol.[49] We have previously demonstrated that Y731F AAV-9 resulted in efficient local and systemic gene transfer in DMD dog muscle.[9,10] The viral titer was determined using the Fast SYBR Green Master Mix kit (Bio-Rad, Hercules, CA, USA) by real-time quantitative PCR (qPCR) in an ABI 7900 HT qPCR machine (Applied Biosystems, Foster City, CA, USA). The forward primer was 5′-TTACGGTAAACTGCCCACTTG-3′. The reverse primer was 5′-CATAAGGTCATGTACTGGGCATAA-3′.

AAV delivery

The intramuscular injection was performed under transient immune suppression according to our published protocol.[9,15] Specifically, transient immunosuppression was applied 1 week before AAV injection and continued for 5 weeks (i.e., 4 weeks after injection). Cyclosporine (Neoral, 100 mg/mL; Novartis, East Hanover, NJ, USA; NDC 0078-0274-22) and mycophenolate mofetil (CellCept, 200 mg/mL; Genentech, South San Francisco, CA, USA; NDC 0004-0261-29) were used to achieve immunosuppression. Cyclosporine was administered orally at 10–20 mg/kg/day to achieve a whole blood trough level of 100–200 ng/mL. The cyclosporine level was measured at the Clinical Pathology Laboratory in the University of Missouri Hospital (Columbia, MO, USA). The blood trough level

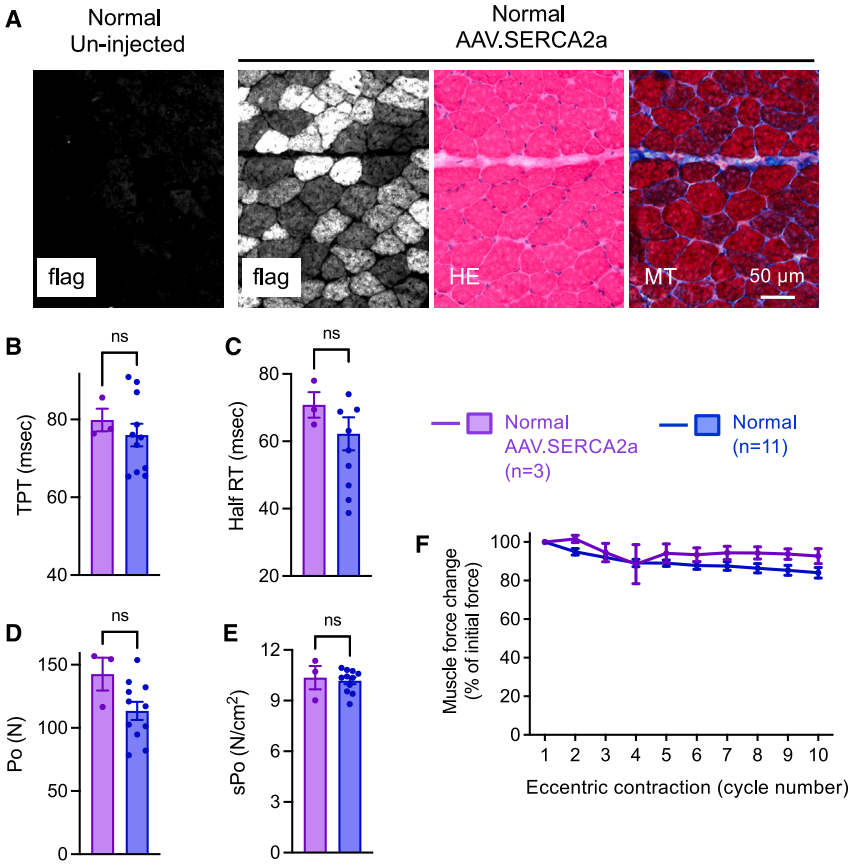

Figure 6. AAV.SERCA2a injection did not alter the histology or function of normal dog muscle

(A) Representative photomicrographs of FLAG tag immunofluorescence staining, H&E staining, and Masson trichrome (MT) staining. (B) Quantification of time to peak tension (TPT) of twitch contraction. (C) Quantification of half relaxing time (Half RT) of twitch contraction. (D) Quantification of total tetanic muscle force (Po). (E) Quantification of specific tetanic muscle force (sPo). (F) Relative changes of the tetanic force during ten cycles of eccentric contraction. The tetanic force at the beginning of the first cycle of eccentric contraction was designated as 100%. Error bar, standard error of the mean. ns, $p > 0.05$.

was achieved on day 6 after starting cyclosporine. Mycophenolate mofetil was administered orally twice daily at 20 mg/kg (40 mg/kg/day).

The dogs were awake and conscious throughout the injection. Briefly, the dogs were gently restrained on the surgery table, and the ECU muscle was identified according to anatomical markings as we have previously described.[9] A total of 7.83×10^{13} viral genome particles were delivered to one side of the ECU muscle (except for one normal dog, which received AAV.SERCA2a on both sides) in a total volume of 2.5 mL. An equal volume of excipient (HEPES buffer) was injected into the contralateral ECU muscle in four affected dogs. SERCA2a expression, muscle histology, and muscle function were examined 12 weeks after AAV injection (except for the normal dog that received AAV.SERCA2a on both sides of the ECU muscle; this dog was examined at 38 weeks after AAV injection).

Morphological studies

Freshly collected muscle samples were embedded in Tissue-Plus optimal cutting temperature media (Scigen Scientific, Gardena, CA, USA) and snap frozen in 2-methylbutane with liquid nitrogen. 10 μm cryosections were used for staining. Slides were viewed at the identical exposure setting using a Nikon E800 fluorescence microscope. Photomicrographs were taken with a QImage Retiga 1300 camera. Immunofluorescence staining was carried out according to previously published protocols.[26] FLAG-tagged human SERCA2a was evaluated by immunostaining using a monoclonal antibody against the FLAG tag (1:500; Sigma-Aldrich, St. Louis, MO, USA, cat. no. F1804, clone M2). Laminin was detected with a polyclonal antibody (1:200; Sigma-Aldrich, cat. no. L9393).[8]

General histology was examined by H&E staining. Fibrosis was examined by Masson trichrome staining using Epredia Richard-Allan Scientific Masson Trichrome Kit (Thermo Fisher Scientific, Waltham, MA, USA, cat. no. 22-110-648).[26] Myosin heavy-chain isoform-dependent muscle-fiber-type distribution was determined with mouse monoclonal antibodies against type I (1:20; DSHB, University of Iowa, Iowa City, IA, USA, cat. no. BA-D5-s), type IIa (1:100; DSHB, University of Iowa, cat. no. SC-71-s), and type IIb (1:40; DSHB, University of Iowa, cat. no. BF-F3-s).[16]

Centrally nucleated myofibers were determined from H&E-stained images using the Fiji imaging software (https://fiji.sc, National Institutes of Health, Bethesda, MD, USA). On average, 2,021 ± 439 myofibers were quantified for each muscle. The fibrotic area was quantified using the lasso tool in the Adobe Photoshop software on Masson trichrome-stained images. Briefly, the micrometer scale was defined with the set measurement scale option in the software. The fibrotic area was marked using the quick selection tool. The sum of all fibrotic areas was then represented as a percentage of the entire image. At least eight different 10× images were quantified for each muscle. The myofiber size (cross-sectional area) was quantified using digitized laminin-stained images using the MyoVision automated image analysis software.[50] On average, 717 ± 65 myofibers were quantified for each muscle. The percentage of fiber-type isoforms was determined from myosin heavy-chain triple immunostaining/laminin co-stained muscle section using the Fiji imaging software (https://fiji.sc). Specifically, a photomicrograph from each muscle section was taken with the UV-2A (blue), TRITC (red), and FITC (green) fluorescence filters. Different fiber types were distinguished based on intracellular color, specifically blue for type I fiber, red for type IIa fiber, and magenta

Table 2. Characterization of the ECU muscle of normal dogs

Weight (g)	Length (cm)	PCSA (cm^2)
AAV.SERCA2a injected		
9.60	16.50	14.42
9.20	16.50	13.82
7.56	14.50	12.92
Untreated normal control		
3.47	12.00	7.17
3.67	11.00	8.27
3.61	10.00	8.95
7.70	18.00	10.60
8.94	15.50	14.29
8.97	17.00	13.07
6.83	15.50	10.92
6.09	13.50	11.18
8.50	16.50	12.77
7.26	14.50	12.41
9.68	18.00	13.33

PCSA, physiological cross-sectional area.

for type I/IIa hybrid fiber. Each type was manually counted using the cell counter plugin module in the software. The total number of fibers was calculated from the sum of each fiber type count. The percentage of each fiber type was determined by dividing the individual fiber type count by the total number of fibers. On average, 1,792 ± 339 myofibers were quantified for each muscle.

Immunohistochemistry staining was used to detect CD4+ T cells, CD8+ T cells, and FoxP3+ nuclei, according to our established protocols.[35,46] Specifically, CD4+ T cells were detected using a rat monoclonal IgG2a antibody against canine CD4 (1:1000; Bio-Rad, cat. no. MCA1038GA, clone YKIX 302.9). CD8+ T cells were detected using a rat monoclonal IgG1 antibody against canine CD8 (1:200; Bio-Rad, cat. no. MCA1039, clone YCATE 55.9). FoxP3+ nuclei were detected using a rat monoclonal IgG2a antibody against mouse FoxP3 (1:200; Thermo Fisher Scientific, cat. no. 14–5773, clone FJK-16s).

AAV vector genome copy-number quantification

Genomic DNA was extracted from OCT-embedded tissue samples. DNA concentration was quantified with Qubit dsDNA HS assay kit (Thermo Fisher Scientific). The AAV copy number was determined using the PowerUp SYBR Green Master Mix kit (Thermo Fisher Scientific) by real-time qPCR using the QuantStudio 5 Real-Time PCR System (Applied Biosystems). The forward primer was 5′-TTACGG TAAACTGCCCACTTG-3′. The reverse primer was 5′-CATAAG GTCATGTACTGGGCATAA-3′. The linearized AAV.SERCA2a *cis*-plasmid was used to generate the standard curve. The copy number was normalized to diploid genome equivalents using the mean dog c-value of 3.12 pg/haploid genome.[51]

Western blot

Western blot analysis was carried out with whole muscle lysate preparations as described before.[52] SERCA2a was detected using a rabbit polyclonal antibody (1:2,500; Badrilla, Leeds, UK, cat. no. A010-23S). The FLAG tag was detected with a mouse monoclonal antibody (1:500 Sigma, cat. no. F1804, clone M2). α-Tubulin was detected with a mouse monoclonal antibody (1:3,000; Sigma-Aldrich, cat. no. T5168). Western blot quantification was performed using the LI-COR Image Studio v.5.0.21 software (https://www.licor.com). The intensity of the respective protein band was normalized to the corresponding loading control in the same blot.

Sarcoplasmic reticulum Ca^{2+} uptake

SR calcium-dependent calcium uptake was measured following the Millipore filtration technique as previously described.[23] Briefly, about 100–200 μg of the total protein extract was incubated at 37°C in 1.5 mL of calcium uptake medium (in mmol/L, 40 imidazole [pH 7.0], 100 KCl, 5 MgCl2, 5 NaN3, 5 potassium oxalate, and 0.5 EGTA) and various concentrations of $CaCl_2$ to yield 0.03–3 μmol/L free calcium (containing 1 μCi/μmol $^{45}Ca^{2+}$). To obtain the maximal stimulation of SR Ca^{2+} uptake, ruthenium red was added to a final concentration of 1 μM immediately prior to the addition of the substrates to begin calcium uptake. The reaction was initiated by adding ATP to a final concentration of 5 mM and terminated at 1 min by filtration. Each assay was performed in duplicate. The rate of SR Ca^{2+} uptake was determined by non-linear curve fitting analysis using GraphPad Prism v.7.0 software.

Calpain assay

Activated calpain was measured in protein lysates from muscle tissue using a fluorometric calpain activity assay kit (Abcam, Cambridge, MA, USA, cat. no. ab65308) according to the manufacturer's instructions. Briefly, cytosolic protein extracts were prepared with the provided extraction buffer, which prevented auto-activation of calpain during the extraction procedure, enabling the detection of only activated calpain in the cytosol. The calpain activity was measured using a fluorometric assay to detect cleavage of calpain substrate Ac-LLY-AFC. The calpain activity is reported as relative fluorescence units/mg protein.

Muscle force measurements

The ECU muscle force was evaluated according to our previously published protocol.[16,17] Body hair in the surgical areas was shaved, and skin was disinfected with 70% ethanol. Anesthesia was first induced by intravenous injection of propofol (6 mg/kg), the subject was then intubated, and anesthesia was maintained with 2%–4% isoflurane throughout the experiment. The dogs were placed in a dorsal recumbency position on a custom-made *in situ* muscle function assay setup.[16,17] Respiration was maintained using a mechanical ventilator (Ohmeda 7000, Ohmeda, Madison, WI, USA) throughout the experiment. The tidal volume was set at 10 mL/min/kg body weight, and the breathing rate was set at 12–15 per min to achieve the partial pressure of carbon dioxide (CO_2) between 35 and 42 mm Hg. The body temperature was maintained at 37°C using two conductive blankets

(Adroit Medical Systems, Loudon, TN, USA) connected to a heated circulating water bath (Thermo, Fisher Scientific, Hampton, NH, USA). One was placed underneath the animal while the other was placed on top of the animal throughout the experiment. Heart rate, electrocardiograph, oxygen saturation (SpO_2), CO_2, blood pressure, and body temperature were monitored with a veterinary vital sign monitor (DRE Waveline Touch, DRE Veterinary, Louisville, KY, USA) throughout the entire experiment. Vital signs, capillary refill time, mucous membrane color, the palpebral reflex, and the pedal reflex were recorded every 15 min.

A catheter (The BD Insyte Autoguard Shielded IV Catheters, 20G × 1.00″, Becton Dickinson, Franklin Lakes, NJ, USA) was inserted into the saphenous vein for intravenous saline infusion (Vetivex sodium chloride injection solution 0.9%, Dechra Veterinary Products, Overland Park, KS, USA). The infusion rate was set to 4 mL/kg/h. The skin between the medial and lateral sides of the neck was disinfected with 70% ethanol, and a 4–6 cm segment of the right carotid artery was surgically exposed. The proximal end of the artery was tied with a 2-0 braided silk suture (Surgical Specialties, Wyomissing, PA, USA) to block the blood flow. A small incision was made in the artery, and a silicone tube (outer diameter: 1.8 mm, and inner diameter: 1.0 mm) was inserted and advanced to the thoracic aorta to measure the central blood pressure. The tube was then secured to the carotid artery using a 2-0 braided silk suture (Surgical Specialties), and the skin incision site was closed with a 4-0 braided silk suture (Surgical Specialties).

The ECU muscle force was measured using the 310C-LR Dual-Mode lever system (Aurora Scientific, Aurora, ON, Canada). Briefly, the entire ECU muscle was surgically exposed, and the distal tendon was attached to the force transducer (Model #6400, Cambridge Technology, Lexington, MA, USA). A temperature probe (YSI 400, Yellow Springs Instrument, Yellow Springs, OH, USA) was placed between the ECU muscle and the radius bone to monitor the muscle temperature throughout the experiment. The exposed ECU muscle and tendon were covered with warm, wet saline gauze and then covered with Saran Wrap to avoid moisture evaporation. The radial nerve was carefully dissected and mounted on a stimulator (Model #701A, Aurora Scientific). The 310C-LR Dual-Mode lever system was connected to a PC using an interface (Model #604A, Aurora Scientific), and it was controlled by the Dynamic Muscle Control software (v.5.420, Aurora Scientific). The controller module was configured by the manufacturer for isometric and eccentric contractions. The muscle force was recorded and analyzed using the Dynamic Muscle Analysis software (v.5.321, Aurora Scientific).

The ECU muscle was first stimulated three times at 150 Hz and 10 mA for 200 ms with a 60 s rest between each stimulus to warm up the muscle.[53,54] The optimal resting tension, current, and stimulation duration were determined using our published protocol.[16] To determine the absolute tetanic force (Po), the muscle was stimulated using the optimal current and optimal duration at different frequencies (5, 20, 40, 60, 80, 100, and 120 Hz). The highest muscle force was defined as Po. After a 2 min rest, the muscle was set at the optimal resting tension and stimulated at 1 Hz using the optimal current to study twitch contraction kinetics. After 2 min rest, the ECU muscle was subjected to 10 repetitive cycles of eccentric contraction. The muscle was rested for 1 min between two consecutive eccentric cycles. The specific tetanic force (sPo) was calculated by dividing the Po by the muscle pCSA. The pCSA was calculated according to the equation: (muscle weight in g × cos10.03°)/(1.056 g/cm^3 × Lf in cm).[55] 10.03° is the average pennation angle of the ECU muscle.[55] 1.0597 g/cm^3 is the muscle density.[56] Lf is the optimal fiber length. Lf was determined by multiplying the measured muscle length by the fiber length/muscle length ratio. This ratio is 0.0448 for the ECU muscle.[55] The percentage of force drop during eccentric contraction was calculated according to our published protocol.[54,55,57] The dogs were euthanized at the end of the assay, and tissues were collected for further analysis.

Statistical analysis

Data are presented as mean ± standard error of the mean. All statistical analyses were performed using GraphPad PRISM software v.9.1.1 (GraphPad Software, La Jolla, CA, USA). Data were checked with the Shapiro-Wilk test to confirm normality. To compare the statistical significance between AAV.SERCA2a-injected and contralateral excipient-injected muscle in affected dogs, the paired Student's t test was used for parametric data, and the Wilcoxon signed-rank test was used for non-parametric data. To compare the statistical significance between AAV.SERCA2a-injected and uninjected normal dog muscle, the unpaired Student's t test was used for parametric data, and the Mann-Whitney test was used for non-parametric data. Two-way ANOVA with Tukey's multiple comparison tests was carried out for three-group comparisons in Figure 2A. One-way ANOVA with Tukey's multiple comparison tests was carried out for three-group comparisons in Figures 2B and 2C. A p value of less than 0.05 was considered statistically significant.

DATA AND CODE AVAILABILITY

The data presented in this study are available from the corresponding author upon reasonable request.

SUPPLEMENTAL INFORMATION

Supplemental information can be found online at https://doi.org/10.1016/j.omtm.2024.101268.

ACKNOWLEDGMENTS

This work was supported by grants from the National Institutes of Health AR-70517 (to D.D. and G.J.B.) and AI-177600 (to R.W.H. and D.D.), Jesse Davidson Foundation-Defeat Duchenne Canada (to D.D. and G.J.B.), and the Jackson Freel DMD Research Fund (to D.D.). The authors thank Dr. Arun Srivastava (University of Florida) for sharing the tyrosine-mutated AAV9 capsid packaging plasmid.

AUTHOR CONTRIBUTIONS

D.D. conceived the idea and designed the study. K.K., C.H.H., M.J.B., Y.Y., J.A.T., and G.J.B. conducted experiments. K.K., C.H.H., M.J.B.,

G.Y., G.J.B., R.W.H., and D.D. analyzed the data. K.K. and D.D. wrote the paper. All authors edited the paper and approved the submission.

DECLARATION OF INTERESTS

D.D. is a member of the scientific advisory board for Solid Biosciences and an equity holder of Solid Biosciences. D.D. is a member of the scientific advisory board for Sardocor Corp. D.D. is an inventor of several issued and filed patents on AAV vector and DMD gene therapy. The Duan lab has received research support unrelated to this project from Elenae Therapeutics and Satellos Bioscience in the last 3 years. R.W.H. is serving on scientific advisory boards for the Regeneron Pharmaceuticals-Intellia Therapeutics collaboration, Prevail Therapeutics, Pfizer, and Biomarin and is also receiving funding from Roche.

REFERENCES

1. Duan, D., Goemans, N., Takeda, S., Mercuri, E., and Aartsma-Rus, A. (2021). Duchenne muscular dystrophy. Nat. Rev. Dis. Primers *7*, 13. https://doi.org/10.1038/s41572-021-00248-3.
2. Mareedu, S., Million, E.D., Duan, D., and Babu, G.J. (2021). Abnormal calcium handling in Duchenne muscular dystrophy: mechanisms and potential therapies. Front. Physiol. *12*, 647010.
3. Turner, P.R., Westwood, T., Regen, C.M., and Steinhardt, R.A. (1988). Increased protein degradation results from elevated free calcium levels found in muscle from mdx mice. Nature *335*, 735–738. https://doi.org/10.1038/335735a0.
4. Fong, P.Y., Turner, P.R., Denetclaw, W.F., and Steinhardt, R.A. (1990). Increased activity of calcium leak channels in myotubes of Duchenne human and mdx mouse origin. Science *250*, 673–676.
5. Periasamy, M., and Kalyanasundaram, A. (2007). SERCA pump isoforms: their role in calcium transport and disease. Muscle Nerve *35*, 430–442. https://doi.org/10.1002/mus.20745.
6. Toyoshima, C. (2009). How Ca2+-ATPase pumps ions across the sarcoplasmic reticulum membrane. Biochim. Biophys. Acta *1793*, 941–946. https://doi.org/10.1016/j.bbamcr.2008.10.008.
7. Shin, J.-H., Bostick, B., Yue, Y., Hajjar, R., and Duan, D. (2011). SERCA2a gene transfer improves electrocardiographic performance in aged mdx mice. J. Transl. Med. *9*, 132. https://doi.org/10.1186/1479-5876-9-132.
8. Wasala, N.B., Yue, Y., Lostal, W., Wasala, L.P., Niranjan, N., Hajjar, R.J., Babu, G.J., and Duan, D. (2020). Single SERCA2a Therapy Ameliorated Dilated Cardiomyopathy for 18 Months in a Mouse Model of Duchenne Muscular Dystrophy. Mol. Ther. *28*, 845–854. https://doi.org/10.1016/j.ymthe.2019.12.011.
9. Shin, J.-H., Pan, X., Hakim, C.H., Yang, H.T., Yue, Y., Zhang, K., Terjung, R.L., and Duan, D. (2013). Microdystrophin ameliorates muscular dystrophy in the canine model of Duchenne muscular dystrophy. Mol. Ther. *21*, 750–757. https://doi.org/10.1038/mt.2012.283.
10. Yue, Y., Pan, X., Hakim, C.H., Kodippili, K., Zhang, K., Shin, J.-H., Yang, H.T., McDonald, T., and Duan, D. (2015). Safe and bodywide muscle transduction in young adult Duchenne muscular dystrophy dogs with adeno-associated virus. Hum. Mol. Genet. *24*, 5880–5890.
11. Duan, D. (2015). Duchenne muscular dystrophy gene therapy in the canine model. Hum. Gene Ther. Clin. Dev. *26*, 57–69. https://doi.org/10.1089/humc.2015.006.
12. Kodippili, K., Hakim, C.H., Pan, X., Yang, H.T., Yue, Y., Zhang, Y., Shin, J.H., Yang, N.N., and Duan, D. (2018). Dual AAV gene therapy for Duchenne muscular dystrophy with a 7-kb mini-dystrophin gene in the canine model. Hum. Gene Ther. *29*, 299–311. https://doi.org/10.1089/hum.2017.095.
13. Birch, S.M., Lawlor, M.W., Conlon, T.J., Guo, L.J., Crudele, J.M., Hawkins, E.C., Nghiem, P.P., Ahn, M., Meng, H., Beatka, M.J., et al. (2023). Assessment of systemic AAV-microdystrophin gene therapy in the GRMD model of Duchenne muscular dystrophy. Sci. Transl. Med. *15*, eabo1815. https://doi.org/10.1126/scitranslmed.abo1815.
14. McGreevy, J.W., Hakim, C.H., McIntosh, M.A., and Duan, D. (2015). Animal models of Duchenne muscular dystrophy: from basic mechanisms to gene therapy. Dis. Model. Mech. *8*, 195–213. https://doi.org/10.1242/dmm.018424.
15. Shin, J.-H., Yue, Y., Srivastava, A., Smith, B., Lai, Y., and Duan, D. (2012). A simplified immune suppression scheme leads to persistent micro-dystrophin expression in Duchenne muscular dystrophy dogs. Hum. Gene Ther. *23*, 202–209. https://doi.org/10.1089/hum.2011.147.
16. Hakim, C.H., Yang, H.T., Burke, M.J., Teixeira, J., Jenkins, G.J., Yang, N.N., Yao, G., and Duan, D. (2021). Extensor carpi ulnaris muscle shows unexpected slow-to-fast fiber type switch in Duchenne muscular dystrophy dogs. Dis. Model. Mech. *14*, dmm049006. https://doi.org/10.1242/dmm.049006.
17. Hakim, C.H., Teixeira, J., Leach, S.B., and Duan, D. (2023). Physiological Assessment of Muscle, Heart, and Whole Body Function in the Canine Model of Duchenne Muscular Dystrophy. Methods Mol. Biol. *2587*, 67–103. https://doi.org/10.1007/978-1-0716-2772-3_5.
18. Lin, B.L., Shin, J.Y., Jeffreys, W.P., Wang, N., Lukban, C.A., Moorer, M.C., Velarde, E., Hanselman, O.A., Kwon, S., Kannan, S., et al. (2022). Pharmacological TRPC6 inhibition improves survival and muscle function in mice with Duchenne muscular dystrophy. JCI Insight *7*, e158906. https://doi.org/10.1172/jci.insight.158906.
19. Capogrosso, R.F., Mantuano, P., Uaesoontrachoon, K., Cozzoli, A., Giustino, A., Dow, T., Srinivassane, S., Filipovic, M., Bell, C., Vandermeulen, J., et al. (2018). Ryanodine channel complex stabilizer compound S48168/ARM210 as a disease modifier in dystrophin-deficient mdx mice: proof-of-concept study and independent validation of efficacy. FASEB J. *32*, 1025–1043. https://doi.org/10.1096/fj.201700182RRR.
20. Nogami, K., Maruyama, Y., Sakai-Takemura, F., Motohashi, N., Elhussieny, A., Imamura, M., Miyashita, S., Ogawa, M., Noguchi, S., Tamura, Y., et al. (2021). Pharmacological activation of SERCA ameliorates dystrophic phenotypes in dystrophin-deficient mdx mice. Hum. Mol. Genet. *30*, 1006–1019. https://doi.org/10.1093/hmg/ddab100.
21. Morine, K.J., Sleeper, M.M., Barton, E.R., and Sweeney, H.L. (2010). Overexpression of SERCA1a in the mdx diaphragm reduces susceptibility to contraction-induced damage. Hum. Gene Ther. *21*, 1735–1739. https://doi.org/10.1089/hum.2010.077.
22. Goonasekera, S.A., Lam, C.K., Millay, D.P., Sargent, M.A., Hajjar, R.J., Kranias, E.G., and Molkentin, J.D. (2011). Mitigation of muscular dystrophy in mice by SERCA overexpression in skeletal muscle. J. Clin. Invest. *121*, 1044–1052. https://doi.org/10.1172/JCI43844.
23. Voit, A., Patel, V., Pachon, R., Shah, V., Bakhutma, M., Kohlbrenner, E., McArdle, J.J., Dell'Italia, L.J., Mendell, J.R., Xie, L.H., et al. (2017). Reducing sarcolipin expression mitigates Duchenne muscular dystrophy and associated cardiomyopathy in mice. Nat. Commun. *8*, 1068. https://doi.org/10.1038/s41467-017-01146-7.
24. Morales, E.D., Yue, Y., Watkins, T.B., Han, J., Pan, X., Gibson, A.M., Hu, B., Brito-Estrada, O., Yao, G., Makarewich, C.A., et al. (2023). Dwarf Open Reading Frame (DWORF) Gene Therapy Ameliorated Duchenne Muscular Dystrophy Cardiomyopathy in Aged mdx Mice. J. Am. Heart Assoc. *12*, e027480. https://doi.org/10.1161/JAHA.122.027480.
25. Schneider, J.S., Shanmugam, M., Gonzalez, J.P., Lopez, H., Gordan, R., Fraidenraich, D., and Babu, G.J. (2013). Increased sarcolipin expression and decreased sarco(endo) plasmic reticulum Ca2+ uptake in skeletal muscles of mouse models of Duchenne muscular dystrophy. J. Muscle Res. Cell Motil. *34*, 349–356. https://doi.org/10.1007/s10974-013-9350-0.
26. Hakim, C.H., Burke, M.J., Teixeira, J., and Duan, D. (2023). Histological Assessment of Gene Therapy in the Canine DMD Model. Methods Mol. Biol. *2587*, 303–338. https://doi.org/10.1007/978-1-0716-2772-3_16.
27. Greenberg, B., Butler, J., Felker, G.M., Ponikowski, P., Voors, A.A., Desai, A.S., Barnard, D., Bouchard, A., Jaski, B., Lyon, A.R., et al. (2016). Calcium upregulation by percutaneous administration of gene therapy in patients with cardiac disease (CUPID 2): a randomised, multinational, double-blind, placebo-controlled, phase 2b trial. Lancet *387*, 1178–1186. https://doi.org/10.1016/S0140-6736(16)00082-9.
28. Hulot, J.S., Salem, J.E., Redheuil, A., Collet, J.P., Varnous, S., Jourdain, P., Logeart, D., Gandjbakhch, E., Bernard, C., Hatem, S.N., et al. (2017). Effect of intracoronary administration of AAV1/SERCA2a on ventricular remodelling in patients with advanced systolic heart failure: results from the AGENT-HF randomized phase 2 trial. Eur. J. Heart Fail. *19*, 1534–1541. https://doi.org/10.1002/ejhf.826.

29. Lyon, A.R., Babalis, D., Morley-Smith, A.C., Hedger, M., Suarez Barrientos, A., Foldes, G., Couch, L.S., Chowdhury, R.A., Tzortzis, K.N., Peters, N.S., et al. (2020). Investigation of the safety and feasibility of AAV1/SERCA2a gene transfer in patients with chronic heart failure supported with a left ventricular assist device - the SERCA-LVAD TRIAL. Gene Ther. *27*, 579–590. https://doi.org/10.1038/s41434-020-0171-7.

30. Mi, Y.F., Li, X.Y., Tang, L.J., Lu, X.C., Fu, Z.Q., and Ye, W.H. (2009). Improvement in cardiac function after sarcoplasmic reticulum Ca2+-ATPase gene transfer in a beagle heart failure model. Chin. Med. J. *122*, 1423–1428.

31. Zhu, X., McTiernan, C.F., Rajagopalan, N., Shah, H., Fischer, D., Toyoda, Y., Letts, D., Bortinger, J., Gibson, G., Xiang, W., et al. (2012). Immunosuppression decreases inflammation and increases AAV6-hSERCA2a-mediated SERCA2a expression. Hum. Gene Ther. *23*, 722–732. https://doi.org/10.1089/hum.2011.108.

32. Herzog, R.W., Yang, E.Y., Couto, L.B., Hagstrom, J.N., Elwell, D., Fields, P.A., Burton, M., Bellinger, D.A., Read, M.S., Brinkhous, K.M., et al. (1999). Long-term correction of canine hemophilia B by gene transfer of blood coagulation factor IX mediated by adeno-associated viral vector. Nat. Med. *5*, 56–63.

33. Yuasa, K., Yoshimura, M., Urasawa, N., Ohshima, S., Howell, J.M., Nakamura, A., Hijikata, T., Miyagoe-Suzuki, Y., and Takeda, S. (2007). Injection of a recombinant AAV serotype 2 into canine skeletal muscles evokes strong immune responses against transgene products. Gene Ther. *14*, 1249–1260.

34. Mueller, C., Chulay, J.D., Trapnell, B.C., Humphries, M., Carey, B., Sandhaus, R.A., McElvaney, N.G., Messina, L., Tang, Q., Rouhani, F.N., et al. (2013). Human Treg responses allow sustained recombinant adeno-associated virus-mediated transgene expression. J. Clin. Invest. *123*, 5310–5318. https://doi.org/10.1172/JCI70314.

35. Hakim, C.H., Kumar, S.R.P., Pérez-López, D.O., Wasala, N.B., Zhang, D., Yue, Y., Teixeira, J., Pan, X., Zhang, K., Million, E.D., et al. (2021). Cas9-specific immune responses compromise local and systemic AAV CRISPR therapy in multiple dystrophic canine models. Nat. Commun. *12*, 6769. https://doi.org/10.1038/s41467-021-26830-7.

36. Potz, B.A., Abid, M.R., and Sellke, F.W. (2016). Role of Calpain in Pathogenesis of Human Disease Processes. J. Nat. Sci. *2*, e218.

37. Spencer, M.J., Croall, D.E., and Tidball, J.G. (1995). Calpains are activated in necrotic fibers from mdx dystrophic mice. J. Biol. Chem. *270*, 10909–10914.

38. Gokhin, D.S., Tierney, M.T., Sui, Z., Sacco, A., and Fowler, V.M. (2014). Calpain-mediated proteolysis of tropomodulin isoforms leads to thin filament elongation in dystrophic skeletal muscle. Mol. Biol. Cell *25*, 852–865. https://doi.org/10.1091/mbc.E13-10-0608.

39. Gaglianone, R.B., Bloise, F.F., Lagrota-Candido, J., Mermelstein, C., and Quirico-Santos, T. (2021). Persistent mdx diaphragm alterations are accompanied by increased expression and activity of calcium and muscle-specific proteins. Histol. Histopathol. *36*, 775–783. https://doi.org/10.14670/HH-18-334.

40. Selsby, J., Pendrak, K., Zadel, M., Tian, Z., Pham, J., Carver, T., Acosta, P., Barton, E., and Sweeney, H.L. (2010). Leupeptin-based inhibitors do not improve the mdx phenotype. Am. J. Physiol. Regul. Integr. Comp. Physiol. *299*, R1192–R1201. https://doi.org/10.1152/ajpregu.00586.2009.

41. Childers, M.K., Bogan, J.R., Bogan, D.J., Greiner, H., Holder, M., Grange, R.W., and Kornegay, J.N. (2011). Chronic administration of a leupeptin-derived calpain inhibitor fails to ameliorate severe muscle pathology in a canine model of duchenne muscular dystrophy. Front. Pharmacol. *2*, 89. https://doi.org/10.3389/fphar.2011.00089.

42. Petrof, B.J., Shrager, J.B., Stedman, H.H., Kelly, A.M., and Sweeney, H.L. (1993). Dystrophin protects the sarcolemma from stresses developed during muscle contraction. Proc. Natl. Acad. Sci. USA *90*, 3710–3714.

43. Stedman, H.H., Sweeney, H.L., Shrager, J.B., Maguire, H.C., Panettieri, R.A., Petrof, B., Narusawa, M., Leferovich, J.M., Sladky, J.T., and Kelly, A.M. (1991). The mdx mouse diaphragm reproduces the degenerative changes of Duchenne muscular dystrophy. Nature *352*, 536–539.

44. Bish, L.T., Sleeper, M.M., Reynolds, C., Gazzara, J., Withnall, E., Singletary, G.E., Buchlis, G., Hui, D., High, K.A., Gao, G., et al. (2011). Cardiac gene transfer of short hairpin RNA directed against phospholamban effectively knocks down gene expression but causes cellular toxicity in canines. Hum. Gene Ther. *22*, 969–977. https://doi.org/10.1089/hum.2011.035.

45. Law, M.L., Prins, K.W., Olander, M.E., and Metzger, J.M. (2018). Exacerbation of dystrophic cardiomyopathy by phospholamban deficiency mediated chronically increased cardiac Ca(2+) cycling in vivo. Am. J. Physiol. Heart Circ. Physiol. *315*, H1544–H1552. https://doi.org/10.1152/ajpheart.00341.2018.

46. Smith, B.F., Yue, Y., Woods, P.R., Kornegay, J.N., Shin, J.-H., Williams, R.R., and Duan, D. (2011). An intronic LINE-1 element insertion in the dystrophin gene aborts dystrophin expression and results in Duchenne-like muscular dystrophy in the corgi breed. Lab. Invest. *91*, 216–231. https://doi.org/10.1038/labinvest.2010.146.

47. Fine, D.M., Shin, J.-H., Yue, Y., Volkmann, D., Leach, S.B., Smith, B.F., McIntosh, M., and Duan, D. (2011). Age-matched comparison reveals early electrocardiography and echocardiography changes in dystrophin-deficient dogs. Neuromuscul. Disord. *21*, 453–461. https://doi.org/10.1016/j.nmd.2011.03.010.

48. Petrs-Silva, H., Dinculescu, A., Li, Q., Min, S.H., Chiodo, V., Pang, J.J., Zhong, L., Zolotukhin, S., Srivastava, A., Lewin, A.S., and Hauswirth, W.W. (2009). High-efficiency transduction of the mouse retina by tyrosine-mutant AAV serotype vectors. Mol. Ther. *17*, 463–471. https://doi.org/10.1038/mt.2008.269.

49. Shin, J.-H., Yue, Y., and Duan, D. (2012). Recombinant adeno-associated viral vector production and purification. Methods Mol. Biol. *798*, 267–284. https://doi.org/10.1007/978-1-61779-343-1_15.

50. Viggars, M.R., Wen, Y., Peterson, C.A., and Jarvis, J.C. (2022). Automated cross-sectional analysis of trained, severely atrophied, and recovering rat skeletal muscles using MyoVision 2.0. J. Appl. Physiol. *132*, 593–610. https://doi.org/10.1152/japplphysiol.00491.2021.

51. Gregory, T.R. (2024). Animal Genome Size Database. www.genomesize.com.

52. Hakim, C.H., Pérez-López, D., Burke, M.J., Teixeira, J., and Duan, D. (2023). Molecular and Biochemical Assessment of Gene Therapy in the Canine Model of Duchenne Muscular Dystrophy. Methods Mol. Biol. *2587*, 255–301. https://doi.org/10.1007/978-1-0716-2772-3_15.

53. Sheard, P., Paul, A., and Duxson, M. (2002). Intramuscular force transmission. Adv. Exp. Med. Biol. *508*, 495–499.

54. Hakim, C.H., Li, D., and Duan, D. (2011). Monitoring murine skeletal muscle function for muscle gene therapy. Methods Mol. Biol. *709*, 75–89.

55. Yang, H.T., Shin, J.-H., Hakim, C.H., Pan, X., Terjung, R.L., and Duan, D. (2012). Dystrophin deficiency compromises force production of the extensor carpi ulnaris muscle in the canine model of Duchenne muscular dystrophy. PLoS One *7*, e44438.

56. Mendez, J., and Keys, A. (1960). Density and composition of mammalian muscle. Metabolism *9*, 184–188.

57. Hakim, C.H., Wasala, N.B., and Duan, D. (2013). Evaluation of muscle function of the extensor digitorum longus muscle ex vivo and tibialis anterior muscle in situ in mice. J. Vis. Exp. *72*, e50183. https://doi.org/10.3791/50183.